JGR Biogeosciences

RESEARCH ARTICLE
10.1029/2024JG008146

Effects of Hot Versus Dry Vapor Pressure Deficit on Ecosystem Carbon and Water Fluxes

Miriam R. Johnston[1], Mallory L. Barnes[2], Yakir Preisler[3], William K. Smith[4], Joel A. Biederman[5], Russell L. Scott[5], A. Park Williams[6], and Matthew P. Dannenberg[1]

[1]Department of Geographical and Sustainability Sciences, University of Iowa, Iowa City, IA, USA, [2]O'Neill School of Public and Environmental Affairs, Indiana University, Bloomington, IN, USA, [3]Department of Organismic and Evolutionary Biology, Harvard University, Cambridge, MA, USA, [4]School of Natural Resources and the Environment, University of Arizona, Tucson, AZ, USA, [5]U.S. Department of Agriculture, Southwest Watershed Research Center, Agricultural Research Service, Tucson, AZ, USA, [6]Department of Geography, University of California, Los Angeles, CA, USA

Key Points:

- Given values of vapor pressure deficit (VPD) were caused by highly variable combinations of humidity and air temperature across the USA
- Effects of hot/wet *v.* cool/dry VPD differed for both carbon fluxes (half of sites) and water fluxes (35% of sites)
- Flux differences associated with hot *v.* dry VPD varied by site; hotter was often associated with higher carbon fluxes

Supporting Information:

Supporting Information may be found in the online version of this article.

Correspondence to:

M. R. Johnston,
miriam-johnston@uiowa.edu

Citation:

Johnston, M. R., Barnes, M. L., Preisler, Y., Smith, W. K., Biederman, J. A., Scott, R. L., et al. (2025). Effects of hot versus dry vapor pressure deficit on ecosystem carbon and water fluxes. *Journal of Geophysical Research: Biogeosciences*, *130*, e2024JG008146. https://doi.org/10.1029/2024JG008146

Received 15 MAR 2024
Accepted 8 JAN 2025

Abstract Vapor pressure deficit (VPD) has increased and will likely continue increasing, with wide-ranging effects on ecosystems. Future VPD increases will largely be driven by warming, yet most experiments examining VPD effects on plants have done so by changing humidity. Here, we used meteorological data and carbon and water fluxes measured at 26 climatically-diverse eddy covariance sites to quantify the extent to which VPD has been driven by variation in air temperature versus humidity. We fit generalized additive models (GAMs) at each site to quantify effects of hotter (and wetter) and cooler (and drier) versus typical VPD on ecosystem-scale fluxes of carbon and water. We found that VPD has occurred under diverse combinations of temperature and humidity: >50% of a site's daytime growing season temperature range and >35% of its relative humidity range have often combined to define a particular VPD. We found moderate evidence that hotter versus drier VPD of the same magnitude differentially affect gross primary productivity (GPP), net ecosystem productivity (NEP), and latent heat flux (LE): Selected GPP and NEP GAMs at about half of sites and LE GAMs at about a third of sites included a VPD-temperature interaction. The magnitude of the interaction varied, but was generally 29%–57% of the effect attributable solely to VPD. The direction of the interaction also varied, but hot VPD was commonly associated with higher carbon fluxes. These effects were not strongly modified by soil moisture. Overall, results emphasize the relevance of VPD-temperature interactions at a critical time of rapid VPD increase.

Plain Language Summary Plants need water for basic functioning, so the dryness of the air affects many plant processes. A lot of research has focused on how air dryness (aka "vapor pressure deficit" or VPD) affects plant functions such as photosynthesis. However, air can seem dry to plants for two non-exclusive reasons: (a) Moisture is low and/or (b) temperature is high (warm air can hold more moisture, so it will be drier than cool air that has the same amount of moisture). We first asked: At specific locations across the USA, are particular values of VPD always caused by the same combination of temperature and relative humidity? We found that they were not: the same degree of air dryness arises from many combinations of moisture and temperature. We then asked: does this "dryness" versus "hotness" character of VPD matter for plant functioning (net and gross photosynthesis and transpiration of water to the atmosphere)? We report that it is relevant in about half of the ecosystems we studied. Our results emphasize the need to experimentally manipulate VPD by changing moisture and temperature independently to better understand how increasing VPD is affecting plants and ecosystems.

1. Introduction

Vapor pressure deficit (VPD), the difference between saturated and ambient water vapor pressure (Equation 1), defines atmospheric demand for moisture and exerts strong influence on plant structure and function (Grossiord et al., 2020; Olson et al., 2020; Oren et al., 1999; Zweifel et al., 2021). VPD has increased across the majority of the vegetated land surface and likely will continue to increase with further warming (Ficklin & Novick, 2017; Yuan et al., 2019), with potentially acute and varied consequences for ecosystem carbon and water fluxes (Grossiord et al., 2020). In mesic ecosystems, the control exerted by VPD on evapotranspiration and carbon flux may be comparable (Sulman et al., 2016) or even greater (Novick et al., 2016) than the effect of soil

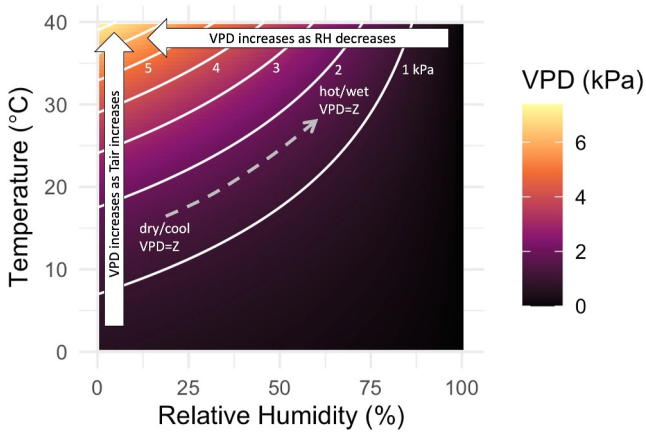

Figure 1. Vapor pressure deficit (VPD) is a function of both temperature and relative humidity, such that diverse combinations of temperature and humidity can result in the same VPD value.

moisture (but see also Liu et al., 2020). In water-limited regions, high VPD depresses primary productivity both following precipitation (Roby et al., 2020) and during extreme drought (Dannenberg et al., 2022). Rising VPD and drying soils can reinforce each other: soil moisture deficit decreases evapotranspiration and increases sensible heat flux, which warms and dries near-surface air and increases VPD that can further dry soils and lead to additional stomatal closure (Zhou et al., 2019). Such amplifying feedbacks between rising VPD and decreasing soil moisture are dominant controls of the interannual variability of the land carbon sink (Humphrey et al., 2021).

An increase in VPD can arise from increased air temperature (Tair), reduced relative humidity (RH), or a combination of the two (Campbell & Norman, 1998; Figure 1). At constant RH, VPD increases exponentially with increasing Tair (via increasing saturated vapor pressure [e_{sat}]; Equations 1 and 2); at constant temperature, VPD decreases linearly with increasing RH (via reduced ambient vapor pressure [e_{amb}]; Equations 1 and 3):

$$\mathrm{VPD} = e_{\mathrm{sat}} - e_{\mathrm{amb}} \tag{1}$$

$$e_{\mathrm{sat}} = 6.1078 \exp\left(\frac{17.08085 * \mathrm{Tair}}{\mathrm{Tair} + 234.175}\right) \tag{2}$$

$$e_{\mathrm{amb}} = \mathrm{RH} * e_{\mathrm{sat}} \tag{3}$$

Varied combinations of temperature and humidity can therefore result in the same VPD, but historical and projected terrestrial VPD trends are driven mostly by increasing temperature (Ficklin & Novick, 2017; Yuan et al., 2019), while RH has remained comparatively stable (or decreased slightly, Q. Zhang et al., 2019).

Here, we primarily refer to elevated VPD conditions as either "hot" or "dry," depending on whether the increased VPD is driven mostly by above-average temperatures (which elevates VPD via increased e_{sat}) or by below-average RH (which elevates VPD via decreased e_{amb}). However, "hot" VPD could be more accurately termed "hot and wet," and "dry" VPD might better be described as "dry and cool." For instance, a high-temperature VPD of 4 kPa would also be a wet VPD compared to a dry VPD of 4 kPa, which would also have to be cool (Figure 1). We opt for the simpler "hot" and "dry" terms to maintain focus on the major factors driving VPD increases.

Despite the role of temperature as a driver of VPD in a warmer world, the effects of hot versus dry VPD of the same magnitude on ecosystem carbon and water fluxes remain largely unknown (Grossiord et al., 2020; Novick et al., 2024). Most experiments examining VPD's effects on plants and communities have manipulated VPD by changing humidity. For example, experiments seeking to clarify the role of abscisic acid in VPD's influence on stomatal conductance (Lange et al., 1971; Oren et al., 1999) controlled humidity at scales ranging from cuvettes (Assmann et al., 2000; Merilo et al., 2018) to growth chambers and greenhouses (Bauerle et al., 2004; Li & Liu, 2022; McAdam & Brodribb, 2015; McAdam et al., 2016). Humidity treatments have also been applied in experiments targeting VPD's effects on photosynthesis (e.g., Inoue et al., 2021; Shirke, 2004), plant morphology and metabolism (e.g., Lihavainen, Ahonen, et al., 2016; Lihavainen et al., 2017; Lihavainen, Keinänen, et al., 2016), plant water relations (e.g., D. Zhang et al., 2017), and monoculture versus polyculture communities (e.g., Aguirre et al., 2021), among others. We are aware of only a few exceptions in which VPD was manipulated by changing temperature rather than humidity or in which factorial treatments of VPD and temperature were applied, typically focused on one or a few species at a mesocosm or smaller scale (Barron-Gafford et al., 2007; Day, 2000; Schönbeck et al., 2022; Sinclair et al., 2007).

Larger-scale, non-manipulative studies aiming to assess the effects of VPD on ecosystems, such as those using eddy covariance and/or remote sensing, typically evaluate VPD without considering its component temperature and humidity drivers (e.g., Dannenberg et al., 2022; Novick et al., 2016; Sulman et al., 2016; Q. Zhang et al., 2019; Li et al., 2023, but see also Fu et al., 2022; Yuan et al., 2019; Zhong et al., 2023). Studies explicitly

examining the effects of hot versus dry VPD, via VPD-temperature interaction terms in statistical models, for example, are usually considerably narrower in scope (e.g., Marchin et al., 2016; Yadav et al., 2010).

Yet, differences in the effects of hot versus dry VPD on ecosystem carbon and water fluxes are theoretically expected. An interaction between VPD and temperature (wherein the flux response to VPD is modulated by temperature) could occur if temperature and VPD act on different processes underlying the flux. For example, gross primary productivity (GPP) may be limited by stomatal conductance and/or by downstream processes like mesophyll conductance, carboxylation, and ribulose 1, 5-bisphosphate (RuBP) regeneration. Stomatal conductance is strongly responsive to VPD (Lange et al., 1971; Oren et al., 1999), and, to a lesser extent, responsive to temperature (Urban et al., 2017). On the other hand, mesophyll conductance, carboxylation, and RuBP regeneration are highly temperature dependent (von Caemmerer & Evans, 2015; Bernacchi et al., 2001; Bernacchi et al., 2003). Therefore, under unfavorable temperatures, GPP might be relatively insensitive to VPD because it is limited by downstream mechanics and biochemistry. In contrast, under favorable temperatures, the influence of VPD on stomatal conductance could dominate the flux. In addition to the effects of VPD being mediated by temperature, the effects of temperature may also be influenced by VPD. For example, VPD's effect on stomatal conductance can affect photosynthetic optimal temperature (Lin et al., 2012).

Water flux (LE) may also be sensitive to differences between hot versus dry VPD. Given a stomatal aperture, water evaporation from a leaf to the atmosphere is largely controlled by the vapor pressure gradient from the leaf to the surrounding atmosphere (following Fick's Law, Campbell and Norman, 1998). However, temperature, independent from its effect on VPD, influences membrane permeability, cuticular conductance, and the viscosity of water (Sadok et al., 2021), all of which may mediate the direct VPD effect on plant transpiration. For example: Hot VPD is likely to drive faster water evaporation from leaf air spaces than dry VPD of the same magnitude, on account of decreased water viscosity at warmer temperatures. Further, stomatal aperture itself is related to carbon assimilation, which is highly temperature-dependent (e.g., Farquhar et al., 1980).

Our research is motivated by the disconnect between the typical manipulative VPD experiment (VPD change driven by humidity) and the ongoing and future changes to global climate (VPD change driven by warming), along with the associated need to improve mechanistic representation of vegetation responses to VPD in ecosystem models (Fu et al., 2022; Yuan et al., 2019). We first quantified the climatic conditions driving variation in VPD, namely the extent to which similar VPD conditions have been driven by different combinations of temperature and RH, using meteorological data measured at 26 long-term eddy covariance sites representing gradients in vegetation composition and climate. Next, we used generalized additive models (GAMs) to examine the influence of hot versus dry versus typical VPD (of the same magnitudes) on ecosystem carbon and water fluxes (net ecosystem productivity, latent energy flux, GPP).

We hypothesized that the effects of hot versus dry VPD would be separable because (H1) widely variable humidity and air temperature conditions would be measured for relatively invariant values of VPD. While it is clear from the physical relationships between RH, Tair, and VPD (Equations 1–3) that this is plausible, the extent to which it occurs across diverse ecosystems remains unexplored. Further, we hypothesized that (H2) hot versus dry VPD would have a different relationship with ecosystem carbon and water fluxes, as indicated by a significant VPD-temperature interaction in statistical models of the fluxes. Finally, we expected that (H3) an interaction between temperature and VPD would be most relevant to carbon and water fluxes under conditions of relatively medium-to-high soil moisture, when plant functioning tends to be most sensitive to VPD because soil moisture is less limiting (Fu et al., 2022; Novick et al., 2016; Roby et al., 2020).

2. Methods

2.1. Study Sites

We used high-quality, ecosystem-scale observational data from a geographically-diverse eddy covariance tower network, thus bridging the gap between leaf- or plant-level and regional- or global-scale studies. To maximize the ecological representation of study sites and to avoid site selection bias, we considered all 31 non-agricultural, non-wetland AmeriFlux core sites and associated cluster sites as candidates. Of the candidate sites, two (US-Ha2 and US-Ho3) were omitted because their temporal records ended before satellite soil moisture acquisitions, which were used as covariates in statistical analyses. Two additional sites (US-Mpj and US-Me2) were omitted due to recent large mortality events, likely resulting in nonstationary relationships between climate and ecosystem function. One

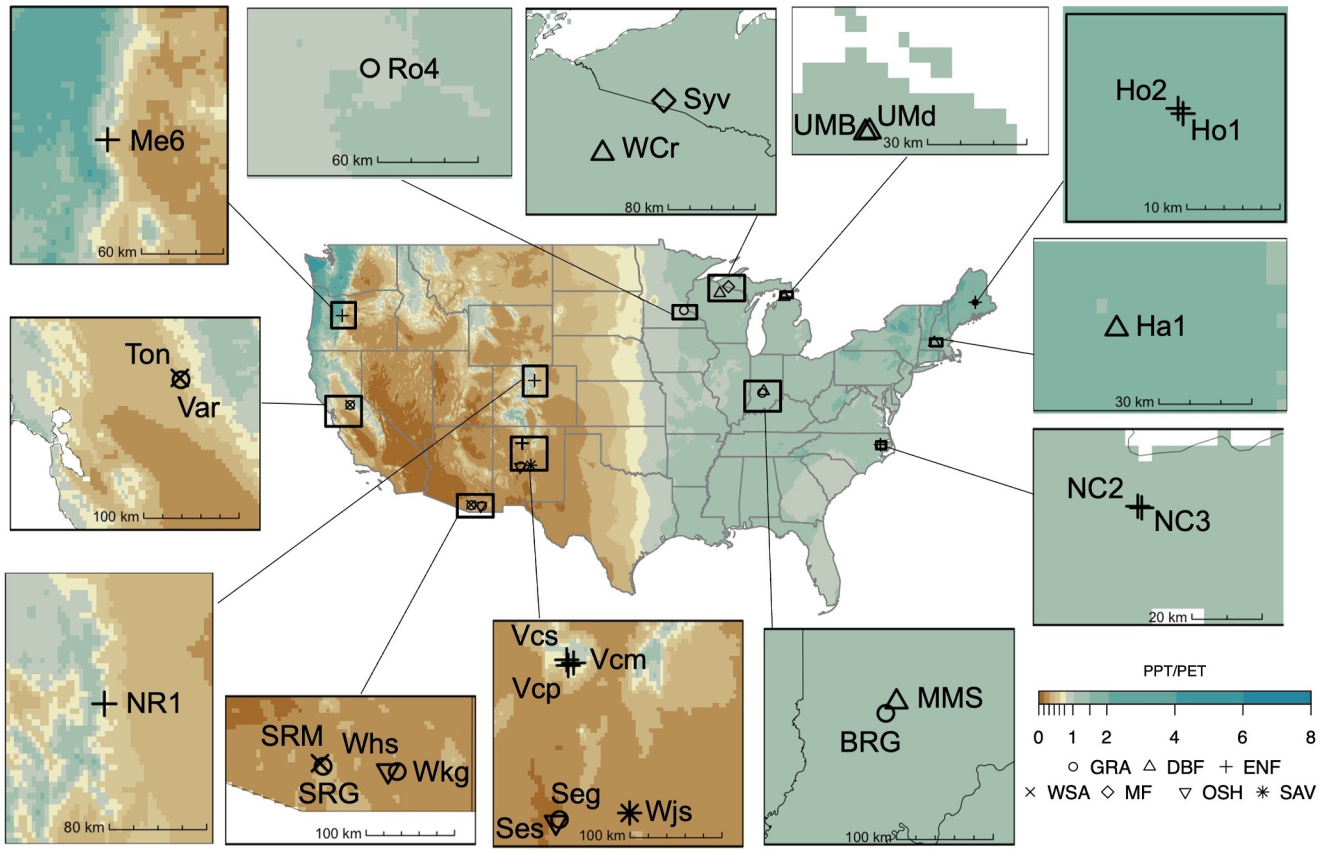

Figure 2. Locations of the 26 focal sites. Points are coded according to the International Geosphere Biosphere Program vegetation scheme (GRA, grassland; DBF, deciduous broadleaf forest; ENF, evergreen needleleaf forest; WSA, woody savanna; MF, mixed forest; OSH, open shrubland; SAV, savanna) and labeled with Ameriflux codes (see Table S1b in Supporting Information S1 for flux site common names). The base map is colored by aridity index (precipitation/potential evapotranspiration; calculated using TerraClimate climatologies, 1981–2010; Abatzoglou et al., 2018).

site (US-PFa) was omitted because its exceptionally high tower (~400 m) results in a highly heterogeneous tower footprint that includes both wetlands and forests. The remaining study sites ($n = 26$) included seven major land cover classes (Figure 2) and spanned a large aridity gradient (Table S1a in Supporting Information S1).

2.2. Data

All data were site-measured or derived from site measurements, with the exception of three-hourly surface (0–5 cm) and root zone (0–100 cm) soil moisture estimates from the 9 km Soil Moisture Active Passive (SMAP) L4 geophysical product (SPL4SMGP version 7, Reichle et al., 2022). SMAP L4 soil moisture estimates are based on assimilation of satellite L-band microwave observations in a land surface hydrology model. While the spatial resolution of SMAP (9 × 9 km) is considerably coarser than most eddy covariance tower footprints (varies, typically 10^3–10^6 km^2; Chu et al., 2021), the resolution of in situ soil moisture sensors is considerably finer than typical tower footprints. As a result, both present representativeness errors in opposite directions, and neither perfectly represents mean soil moisture conditions within the tower footprint. We chose to use SMAP soil moisture estimates because only some AmeriFlux sites measure soil moisture in situ, the number and depths of the soil moisture measurements differ among sites, measurements typically characterize shallower depths than SMAP root zone soil moisture (RZSM) estimates, and the variability of in situ measurements varies across spatial scale and moisture content, making accurate characterization of flux tower footprints non-trivial (Famiglietti et al., 2008). SMAP soil moisture estimates provide a spatially-aggregated, complete record of RZSM from 2015-present, allowing for a consistent representation of the soil profile across sites.

Response variables in statistical models were carbon and water fluxes: net ecosystem productivity (NEP), GPP, and latent energy flux (LE). We obtained NEP and LE from the AmeriFlux network using the "amerifluxr" R

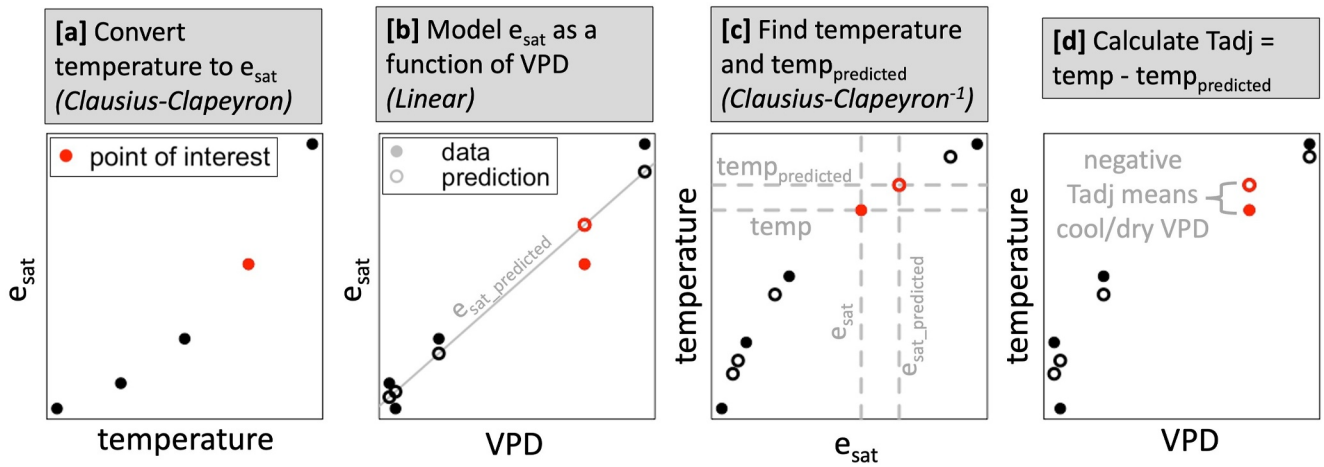

Figure 3. Schematic illustration of Tadj calculation. We interconverted temperature and e_{sat} (a, c) rather than directly modeling temperature as a function of vapor pressure deficit to minimize error associated with calculating residuals of a curved model. The red points are consistent across panels, which is intended to aid intuition.

package (Chu & Hukfens, 2021; R Core Team, 2021). We detected and removed spikes in reported NEP using a spike detection threshold (z) of 5.5 (Equations 2 and 3 in Papale et al., 2006). We then excluded NEP measurements collected during periods of low friction velocity, defined by per-site, per-season thresholds determined via the moving point method implemented in REddyProc (Papale et al., 2006; Wutzler et al., 2018). We gap-filled NEP and LE using the look-up-table approach (Papale et al., 2006) and partitioned NEP into GPP and ecosystem respiration with the night-time partitioning method (Papale et al., 2006; Wutzler et al., 2021). We included only directly measured or high-quality gap-filled data (ReddyProc codes 0 and 1, respectively) in analyses.

As environmental predictors in statistical models, in addition to SMAP RZSM, we used VPD and an adjusted temperature (Tadj) that represents temperature deviation from the expectation for a given VPD at a given site (Figure 3). Briefly, we calculated e_{sat} from observed temperature (Equation 2, Figure 3a) and performed a linear regression of e_{sat} on VPD for each site (Figures 3b, Figure S1 in Supporting Information S1) to calculate the expected e_{sat} at a given value of VPD. We then inverted Equation 2 to calculate the temperature corresponding to the expected e_{sat} (Figure 3c). Tadj was defined as the difference between measured and expected temperature at a given VPD value (Figure 3d). It is positive when temperature is warmer than expected at a given VPD, that is, when VPD is hot (and wet). Conversely, Tadj values are negative when temperature is cooler than expected at a given VPD, that is, when VPD is cool (dry).

We calculated two sets of VPD and Tadj: One based on atmospheric conditions (VPD_a,$Tadj_a$) and one approximating conditions at the leaf surface (VPD_s,$Tadj_s$). The vapor pressure gradient between leaf air spaces and the atmosphere (VPD_s) is a more physiologically-relevant quantity than the VPD of the atmosphere (VPD_a). However, VPD_s is also a more uncertain quantity; it relies on simplistic and assumption-laden estimates of leaf temperature (when calculated via the Stefan-Boltzmann method, used here) or uncertain and dynamic ancillary measurements (Penman-Monteith method). Further, analyses based on VPD_a are likely more broadly generalizable, as VPD_a is more commonly measured and reported by models. We report results from VPD_a analyses in this paper; results based on VPD_s are in Supporting Information S1.

We calculated VPD_a from tower-measured Tair (°C) and RH (%); we calculated VPD_s from RH and surface temperature (Tsurface, °C), obtained via inversion of the Stefan-Boltzmann Law using site-measured longwave radiation, both using the "REddyProc" R package (Wutzler et al., 2021). To calculate emissivity empirically, we also calculated albedo. We used reported measurements from four-way radiometers at the sites to calculate approximate Tsurface (Equations 4–6):

$$\text{Tsurface} = \sqrt[4]{\frac{\text{LWout}}{\sigma\varepsilon}} \quad (4)$$

$$\varepsilon = -0.16\alpha + 0.99 \quad (5)$$

$$\alpha = \frac{\text{SWout}}{\text{SWin}} \tag{6}$$

where LWout is outgoing LW radiation (Wm^{-2}), σ is the Stefan-Boltzmann coefficient ($5.67 \times 10^{-8}\ Wm^{-2}\ K^{-4}$), ε is an estimate of emissivity (Juang et al., 2007), α is albedo, SWout is outgoing SW radiation (Wm^{-2}), and SWin is incoming solar radiation (Wm^{-2}). We then used REddyProc to gap-fill both VPD_a and VPD_s and used only measured or high-quality data in subsequent analyses (Papale et al., 2006).

For all analyses, we filtered data to ensure that relationships among variables were not confounded by seasonal or diurnal effects. We omitted data collected outside of the peak growing season, conservatively defined as days of the year with GPP greater than 80% of maximum GPP, according to a third-order Savitzky-Golay smoother of daily GPP, averaged across years (Figure S2 in Supporting Information S1, Stevens & Ramirez-Lopez, 2022). We further omitted data from times when solar altitude angle was <0.5 radians (28.6°), such that we only considered times of day at which photosynthesis was least likely to be limited by light conditions (R package "suncalc," Thieurmel & Elmarhraoui, 2019). During aphelion, given a relatively hazy atmosphere (transmittance = 0.6), this threshold corresponds to a potential photosynthetic photon flux density (PPFD) of ~800 μmol photons $m^{-2}\ s^{-1}$ (Campbell & Norman, 1998); at other times of year or under higher atmospheric transmittance, potential PPFD would be greater than 800 μmol photons $m^{-2}\ s^{-1}$.

Finally, for the statistical models, we applied wetness and wind filters to avoid error introduced by precipitation, evaporation, and low boundary layer conductance (e.g., Novick et al., 2016; Zhang et al., 2019). Data were omitted if any precipitation occurred at the site in the prior 24 hr, if >5 mm of precipitation occurred in the prior 48 hr, or if soil water content measured at the site or from SMAP surface soil moisture exceeded that of the prior time step by 0.02% or >0.02 vol/vol, respectively. Measurements at times of low wind speed (<1 ms^{-1}) were also removed (Novick et al., 2016; Zhang et al., 2019). Additional details are provided in Table S2 of Supporting Information S1.

2.3. Analyses

2.3.1. Realized Relationships Among VPD, Temperature, and Relative Humidity

To address H1, that variable humidity and air temperature conditions would be measured for relatively invariant values of VPD, we quantified the variability of RH and Tair or Tsurface within narrow bins (width: 0.1 hPa) of VPD_a or VPD_s at each site. We considered measurements and highest-quality filled data during the growing season and growing hours, but did not apply the wetness or wind filter, as these results would not be confounded by wetness or wind (Table S2 in Supporting Information S1). To standardize across the large climatic gradient, we reported ranges of temperature and RH present within VPD bins normalized by the 5th—95th percentile of observed temperature and RH ranges at each site ($n = 26$):

$$\rho_{i,v} = \frac{P_{95}X_{i,b} - P_{05}X_{i,b}}{P_{95}X_i - P_{05}X_i} \tag{7}$$

where i is site, b is VPD bin, X is temperature or RH, P_{95} is the 95th percentile value of X, and P_{05} is the 5th percentile of X. Thus, if $\rho_{i,b} = 1$, then the full range of variability in X measured at site i is present in VPD bin b. Represented proportions of temperature and RH (ρ) were calculated only in the event that >5 data points fell into the VPD bin.

At each site, we fit a loess smoother (span = 0.5) to summarize the relationship between VPD and $\rho_{i,b}$ (R Core Team, 2021; Figure 4). In reporting summary statistics of the smoothers across sites, we include a 95% bootstrap percentile confidence interval (R package "boot," Canty & Ripley, 2021).

2.3.2. Interaction Between VPD, Temperature, and Soil Moisture

To determine whether temperature influenced the relationship between VPD and carbon/water fluxes, we assessed statistical support for an interaction between VPD and Tadj in site-level GAMs (Wood, 2017) of NEP, GPP, and LE. We formulated two sets of models: GPP_s, NEP_s, and LE_s were predicted using models in which

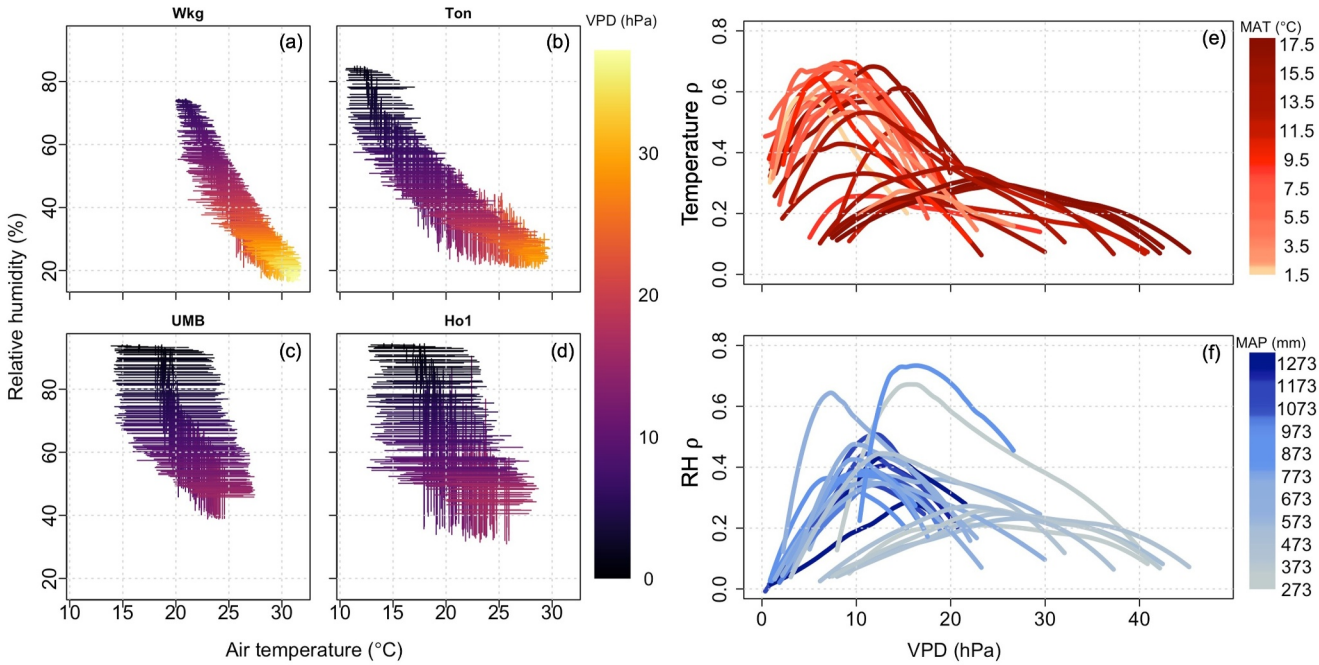

Figure 4. Panels (a–d) show specific ranges of measured relative humidity (RH) and Tair in VPD_a bins of 0.1 hPa at four representative sites, from lowest to highest mean annual precipitation: Wkg (Walnut Gulch Kendall Grasslands) is a grassland, Ton (Tonzi Ranch) is a woody savanna, UMB (University of Michigan Biological Station) is a deciduous broadleaf forest, and Ho1 (Howland forest [main tower]) is an evergreen needleleaf forest. Segments cross at the median air temperature and RH in each vapor pressure deficit bin, and segment length denotes 5th—95th percentiles of half-hourly data. Panels (e, f) show the proportions of a site's 5th–95th percentile Tair and RH ranges (ρ) measured in 0.1 ha VPD_a bins (Equation 7; growing season and growing time only). Each curve is a loess fit to half-hourly (or hourly) data at a single site.

VPD_s and $Tadj_s$ were predictors; GPP_a, NEP_a, and LE_a were predicted using models in which VPD_a and $Tadj_a$ were predictors.

All candidate GAMs were at daily resolution and included an offset for year to accommodate year-to-year variability in baseline conditions (such as leaf area). Additionally, they all included smoothed terms for SMAP RZSM, VPD, Tadj, and the interactions between RZSM and Tadj and between RZSM and VPD. None of the candidate GAMs included terms explicitly quantifying seasonal or diurnal variation (such as day of year or radiation), as our stringent filtering procedures aimed to remove this variability and isolate conditions when light was not a limiting factor (Table S2 in Supporting Information S1). Candidate GAMs either did not include an interaction between VPD and Tadj (Equation 8), included a two-way interaction between VPD and Tadj (Equation 9), or included both a two-way interaction and a three-way interaction with RZSM (Equation 10). Below, parameters and error terms are omitted for clarity:

$$Y \sim \text{Year} + ti(\text{RZSM}) + ti(\text{VPD}) + ti(\text{Tadj}) + ti(\text{RZSM}, \text{Tadj}) + ti(\text{RZSM}, \text{VPD}) \quad (8)$$

$$Y \sim \text{Year} + ti(\text{RZSM}) + ti(\text{VPD}) + ti(\text{Tadj}) + ti(\text{RZSM}, \text{Tadj}) + ti(\text{RZSM}, \text{VPD}) + ti(\text{VPD}, \text{Tadj}) \quad (9)$$

$$Y \sim \text{Year} + ti(\text{RZSM}) + ti(\text{VPD}) + ti(\text{Tadj}) + ti(\text{RZSM}, \text{Tadj}) + ti(\text{RZSM}, \text{VPD}) + ti(\text{VPD}, \text{Tadj}) + ti(\text{VPD}, \text{Tadj}, \text{RZSM}) \quad (10)$$

The response variable, Y, is NEP, LE, or GPP; Year is an unordered factor, and the *ti* notation indicates a tensor product smooth, specified in R package "mgcv" such that the smooth of an interaction excludes the bases of the main effects and accommodates interactions between variables on different scales (Wood, 2017, 2021). We selected the "best" model for each Y at each site according to AIC value (Akaike, 1974); a chosen model was required to have an AIC value >2 units lower than another other candidate with fewer parameters (Burnham & Anderson, 2004). We assessed all selected model fits graphically (Figures S3–S8 in Supporting Information S1).

If the best model included a VPD-Tadj interaction (Equations 9 or 10), we concluded that "hot" and "dry" VPD had different effects on that response variable at that site. To summarize the magnitude and direction of hot versus dry VPD effects, we compared modeled flux responses given hot, dry, and typical VPD conditions. Specifically, for each GAM, VPD was prescribed as observed and Tadj was prescribed at its 95th percentile (hot VPD), at its 5th percentile (dry VPD), or as equal to 0 (typical VPD). This yielded three predictions per GAM, where the response variable was a flux and the predictors each had a variable contribution to that flux across the observed VPD domain, according to their fitted smooths. We report partial predicted responses, that is, the sum of the contributions of VPD and VPD interaction terms (VPD × Tadj, VPD × RZSM, VPD × Tadj × RZSM) to the response variable (GPP, NEP, LE). Partial responses isolate the effect of VPD on the flux, while full responses may be confounded by the effects of other predictor variables.

If a selected GAM included a three-way interaction between VPD, Tadj, and RZSM (Equation 10), we concluded that RZSM mediated the relevance of hot versus dry VPD for a given site and response variable (H3). We quantified that relevance by comparing partial responses to factorial combinations of high/low Tadj and high/low RZSM (high: 95th percentile, low: 5th percentile).

3. Results

3.1. Broadly Variable Humidity and Air Temperature Conditions Exist for Invariant VPDs

The data strongly supported H1 that specific combinations of temperature and humidity vary greatly for a given VPD (Figure 4, Figure S9 in Supporting Information S1). Typically, sites experienced their widest range of Tair and RH at mid-range values of VPD_a (Figures 4e and 4f). The median site peak temperature ρ (i.e., median across sites of the highest represented temperature proportions in VPD_a bins; Equation 7) was 0.58 (95% CI: 0.42, 0.63; Figure 4e). The median peak RH ρ was 0.38 (CI: 0.35, 0.43; Figure 4f). Across sites, peak ρ corresponded to absolute Tair ranges of 3.0–13.1°C and RH ranges of 11.0%–44.7%. The VPD_a value at which a site experienced its most variable Tair was lower than the VPD_a value at which it experienced its most variable RH (Figure S10 in Supporting Information S1; the median VPD_a difference at peak Tair ρ vs. at peak RH ρ was 2.0 hPa, CI: 1.3, 2.2 hPa).

Sites with higher mean annual temperature (MAT) and lower mean annual precipitation (MAP) often (but not always) experienced narrower ranges of temperature and humidity contributing to VPD than more mesic sites (Figure 4). Four of the seven sites with MAT in the top quartile had a peak temperature ρ in the bottom quartile (Spearman correlation between site MAT and peak temperature $\rho = -0.35$); five of the seven sites with MAP in the bottom quartile had peak RH ρ in the bottom quartile (Spearman correlation = 0.20).

3.2. Hot Versus Dry VPD Affect Carbon and Water Fluxes Differently at Many Sites

The data partially supported H2 that hot versus dry VPD of the same magnitude would have different effects on ecosystem carbon and water fluxes. Fifteen of the 26 site GPP_a models (58%), 13 of the NEP_a models (50%), and 9 of the LE_a models (35%) included an interaction between VPD_a and $Tadj_a$ (Figure 5, Table S3 in Supporting Information S1), indicating that the "hotness" or "dryness" of VPD has a significant effect on the fluxes at those sites. There was fair consistency within sites: GPP_a and NEP_a models either both included or both omitted the interaction at 16/26 sites (62%). However, there were no clear patterns in the prevalence of VPD and Tadj interactions based on site climate or vegetation type (Figure 5, Figure S11 in Supporting Information S1).

All other factors being equal, hot VPD_a was associated with higher GPP_a and NEP_a than typical VPD_a at most sites (11/15 and 12/13 sites, respectively, assessed by comparing partial response values at peak density; Figures 6a and 6b). The partial predicted GPP_a associated with a shift from typical to hot VPD ranged from −0.59 to 0.88 $\mu molm^{-2}\ s^{-1}$ across sites (Q1: −0.01, median: 0.15, Q3: 0.28 $\mu molm^{-2}\ s^{-1}$). The partial predicted NEP_a associated with a shift from typical to hot VPD ranged from −0.22 to 1.38 $\mu molm^{-2}\ s^{-1}$ across sites (Q1: 0.03, median: 0.07, Q3: 0.33 $\mu molm^{-2}\ s^{-1}$). As a percent of the peak density partial responses at typical VPD, these differences between hot and typical partial effects were sizable: median 34% for GPP_a and 57% for NEP_a (Table 1). Conversely, there was no consistent directionality of the dry VPD effect on carbon fluxes relative to typical VPD: Peak partial GPP_a and NEP_a at dry VPD were higher than the typical equivalents at about half the sites (9/15 and 6/13, respectively).

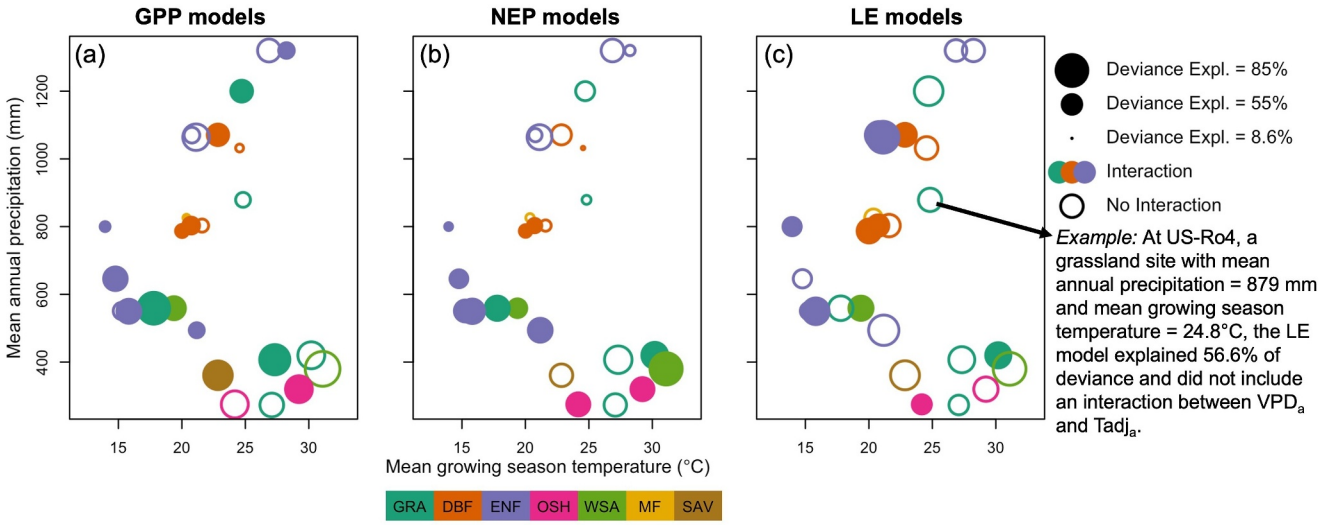

Figure 5. Selected generalized additive models (GAMs) for (a) GPP_a, (b) NEP_a, and (c) LE_a. Filled bubbles indicate that the chosen GAM included an interaction between VPD_a and $Tadj_a$ (Equation 9 or Equation 10); colors denote vegetation type; bubble size is scaled by model deviance explained. There is a single point per site on each panel, plotted in climate space for context. See Figure S11 in Supporting Information S1 for the corresponding figure for models of GPP_s, NEP_s, and LE_s.

Unlike the carbon fluxes, water flux was generally more strongly affected by dry VPD than by hot VPD: partial LE_a at peak density was higher at dry than at typical VPD at 8/9 sites (differences in partial response ranged from −3.16 to 10.83 Wm^{-2}; median difference 4.02 Wm^{-2}; median percentage difference 29%; Figure 6c and Table 1). Beyond these broad patterns, there was remarkably high variability in the effects of hot versus dry versus typical VPD on partial fluxes both across sites and across the range of observed VPD and Tadj (Figures S12–S17 in Supporting Information S1 for surface results).

3.3. Little Evidence That Soil Moisture Mediates the Relevance of Hot Versus Dry VPD

Our third hypothesis, that the hot versus dry quality of VPD would be more relevant under conditions of relatively high soil moisture, was not supported by the GAMs. Only 6 selected GPP_a site models, 5 selected NEP_a models, and 3 selected LE_a models included a three-way interaction between VPD, Tadj, and RZSM (Figures S19 and S20 in Supporting Information S1 for surface), suggesting that at most sites, the value of soil moisture did not modulate the interaction between VPD_a and $Tadj_a$.

4. Discussion

Increased VPD with warming poses severe yet ill-constrained risks to the structure, function, and composition of ecosystems and the services they provide (Grossiord et al., 2020; Lansu et al., 2020; Williams et al., 2013, 2014). One of the key uncertainties in predicting the effects of increasing VPD on vegetation arises from the complex interplay of VPD with temperature and humidity. Theoretically, the same VPD can arise from broadly variable temperature and humidity combinations (Figure 1), but the extent to which that actually occurs was unclear. In this study, we showed that realized values of VPD at AmeriFlux core site clusters correspond to wide ranges of humidity and air temperature (Figure 4). That variability was particularly notable at more mesic sites, where a given value of VPD could occur at more than 50% of a site's daytime growing season temperature and humidity range (Figures 4e and 4f). In other words, across much of the U.S., a single VPD value could arise from a wide range of conditions, from “hot and wet” to “cool and dry.”

We also showed that hot versus dry VPD of the same magnitude can exert distinct effects on carbon and water fluxes across a broad range of ecological settings: we found interactions between VPD and Tadj in approximately half of the models predicting GPP and NEP and in 35% of models predicting LE. These findings challenge the common practice of simplifying VPD into a single, one-dimensional metric, highlight the need to consider the specific factors contributing to VPD change, and should prompt a reassessment of how we approach hot versus dry VPD when modeling ecosystem-level carbon and water fluxes.

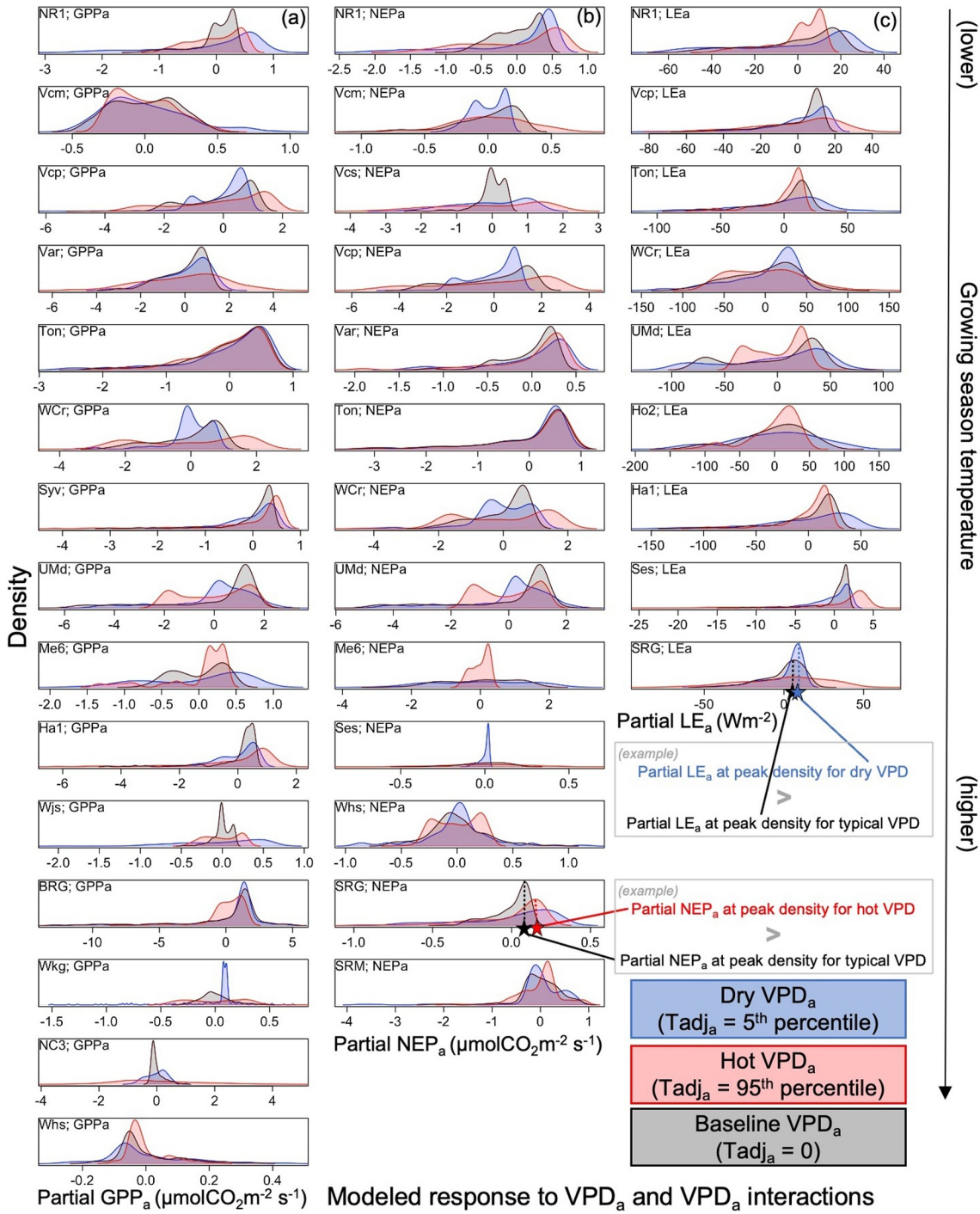

Figure 6. Densities of modeled partial fluxes, that is, the magnitude of the modeled flux [(a) GPP_a, (b) NEP_a, and (c) LE_a] attributable specifically to vapor pressure deficit (VPD) and VPD interaction terms. Only models for which there was a significant VPD_a-$Tadj_a$ interaction ($n = 15$ sites for GPP_a; $n = 13$ for NEP_a; $n = 9$ for LE_a) are shown. Distributions of flux predictions were at observed VPD and year; root zone soil moisture was held at its site median (filtered for growing season, etc.); Tadj was prescribed as the 5th percentile of site Tadj (dry VPD, blue distributions), as the 95th percentile of site Tadj (hot VPD, red distributions) or at Tadj = 0 (neither dry nor hot VPD, black distributions). See Figure S18 in Supporting Information S1 for the corresponding figure for surface analyses. See Table S1b in Supporting Information S1 for common names associated with Ameriflux codes.

Given the theoretical expectation of an interaction between VPD and Tadj, why did we detect a significant interaction for carbon fluxes at only about half the sites, and for water flux at only 35% of the sites? This may be a true representation of reality: if we filtered the data such that temperature was typically favorable, perhaps hot VPD and dry VPD were, in some places, effectively equivalent. However, given the characteristically peaked shape of photosynthetic response to temperature (Berry & Bjorkman, 1980), it is more likely that these results are associated with methodological limitations. First, lagged and cumulative effects of climate on vegetation are widespread (Ding et al., 2020; Ogle et al., 2015), but here we tested the effects of hot versus dry versus typical VPD on concurrent ecosystem fluxes, plausibly depressing the signal of an interaction. Additionally, there are large differences in scale between the leaf-level processes underpinning the theory and the ecosystem-scale fluxes measured by eddy covariance; VPD-temperature interactions evident at the leaf level could be masked by, for example, flux tower footprint heterogeneity (e.g., Barron-Gafford et al., 2007). The presence of species and individuals with different photosynthetic and stomatal sensitivities to temperature, VPD, and other climate factors within a single tower footprint could obfuscate patterns that are species- or individual-specific. Finally, the eddy covariance data, while immensely valuable, are observational; our stringent data filtering attempted to control for confounding environmental and seasonal factors, but it was imperfect and resulted in considerable data loss.

Associated with these challenges and contingencies and corroborating our mixed results, it is unsurprising that the small body of prior studies examining a possible interaction between temperature and VPD on plant functioning has been inconclusive. There was no evidence of a VPD-temperature interaction effect on *Picea rubens* leaf-level net photosynthesis or stomatal conductance in controlled growth chambers (Day, 2000), nor on eddy covariance-based GPP at 8 flux sites, modeled using geostatistical regression (Yadav et al., 2010). While Barron-Gafford et al. (2007) found no significant VPD-temperature interactions for leaf-level fluxes of *Populus deltoides* transpiration and net photosynthesis in controlled mesocosms, the equivalent canopy-scale fluxes were responsive to the interaction. Schönbeck et al. (2022) tested for an interactive effect of VPD and temperature on an array of hydraulic traits of saplings of three species, and found species-specific interactions for a minority of traits. Marchin et al. (2016), applying simple linear regression to model midday transpiration of four hardwood species at Duke Forest, selected models using a quadratic VPD × air temperature predictor about a third of the time. Finally, using a coupled photosynthesis-stomatal conductance model with leaf-level measurements of *Pinus taeda* and *Eucalyptus crebra* net photosynthesis at different temperatures, Lin et al. (2012) found that VPD modulated the optimal photosynthetic temperature.

When statistically significant interactions between VPD and Tadj were detected, hot (and wet) VPD were generally associated with higher GPP_a and NEP_a, while dry (and cool) VPD was generally associated with higher LE_a (Table 1). However, beyond relative locations of distribution peaks (Figure 6), there was large variability in response magnitude and direction across sites. For carbon fluxes, this variability should not be surprising. The expectation is that VPD would have more influence on carbon fluxes when temperature is more favorable (i.e., less limiting to the myriad component processes comprising carbon assimilation). In various conditions and for diverse species, "more favorable" temperature could be either warmer or cooler than ambient, so either warmer or cooler (drier) VPD could be expected to have a larger effect. Similarly, the interaction effect should vary across the range of VPD; at high VPD, for example, stomatal closure would limit carbon fixation, even at favorable temperature (Lange et al., 1971), but the value of "high" VPD would vary by site and by species (Oren et al., 1999). Two to seven years of stringently filtered observational data likely comprised incomplete and idiosyncratic ranges of temperature and VPD conditions at each site, making these intricacies difficult to characterize. In the case of LE flux, we expected more consistent interaction effects, as temperature has monotonic relationships with, for example, water viscosity: at every site, regardless of species or climate, higher temperature decreases the viscosity of water, which would tend to increase transpiration (Sadok et al., 2021). Surprisingly, we found the opposite: Dry VPD, experienced at cooler temperatures, when water should be more viscous, was more consistently associated with high LE flux than hot VPD. Controlled manipulation of VPD and its component temperature and humidity may help to resolve these results.

This research shows that the same value of VPD can arise from a wide range of "hotness" versus "dryness" and presents a strong statistical suggestion that hot versus dry VPD can have different effects on carbon and water fluxes. To extend these results, beyond experimental manipulation, the authors suggest that it may be fruitful to interrogate more temporally complex interactions between VPD and temperature, including lagged and cumulative effects of climate on carbon and water fluxes across a range of time scales (half-hourly, daily, seasonally).

Table 1
Differences Between the Partial Effects of Hot (or Dry) Vapor Pressure Deficit (VPD) (Tadj = 95th or 5th Percentile) and the Partial Effects of Typical VPD (Tadj = 0), Expressed as a Percent of Partial Effects of Typical VPD (Tadj = 0)

Partial response variable *Percent difference calculation; all terms are partial fluxes at peak density* (*see* Figure 6)	Site Q1	Site median	Site Q3	Notable patterns
GPP_a; *100* (hot-typical)/|typical|*	−2%	34%	63%	Hot VPD → higher GPP_a at 11/15 sites
NEP_a; *100* (hot-typical)/|typical|*	14%	57%	131%	Hot VPD → higher NEP_a at 12/13 sites
LE_a; *100* (dry-typical)/|typical|*	12%	29%	35%	Dry VPD → higher LE_a at 8/9 sites

Note. All calculations were performed with site partial fluxes at peak density (see Figure 6). Q1 is the first quartile and Q3 is the third quartile. Note omission of percent difference calculations for partial GPP_a and NEP_a at dry VPD and partial LE_a at hot VPD, on account of no clear patterns. See Table S4 in Supporting Information S1 for corresponding surface calculations.

Additionally, resolving conditions at the leaf surface (VPD_s), which are more physiologically-relevant drivers of plant function, should be a priority. In this study, results of "air" models were broadly comparable to results of canopy "surface" models, but it is difficult to estimate VPD_s at the scale of a flux tower footprint, which integrates a radiative signal from many different plants and exposed soil, and component RH measurements are uncertain due to assumptions of leaf saturation (Cernusak et al., 2018). Additionally, the relevant e_{amb} is that of leaf boundary layers, rather than of the well-mixed atmosphere. More finely resolved measurement of leaf temperature within flux footprints using thermal imagers (e.g., Johnston et al., 2022) could partially assuage these challenges.

5. Conclusion

VPD exerts multifaceted influence on vegetation, with far-reaching consequences for plant physiology and demography. In a warming climate, VPD increases primarily due to temperature change, which exponentially increases the saturation vapor pressure of the atmosphere, resulting in a systematically "hotter" VPD than in a cooler past climate. Our results suggest that consideration of how the changing systematically hotter nature of VPD affects plant function is a priority in the context of global change. Here, we show that realized values of VPD in diverse U.S. ecosystems are frequently characterized by diverse temperature and RH combinations. Furthermore, at about half of the AmeriFlux core cluster sites, VPD has a different effect on ecosystem carbon and/or water fluxes depending on whether it is hotter or drier, even when the VPD itself has the same magnitude. These findings underscore the need to move beyond the one-dimensional view of VPD in both experimental frameworks and predictive models to understand how warming-induced increases in VPD will influence vegetation as climate change progresses.

Data Availability Statement

All raw data used in these analyses are publicly available from the Ameriflux network (https://ameriflux.lbl.gov) or NASA Earthdata (https://search.earthdata.nasa.gov). The relevant code is published on Zenodo (https://doi.org/10.5281/zenodo.14607276).

Acknowledgments
This research was supported by the NASA SMAP Science Team (Grant 80NSSC20K1805) and NSF EPSCoR Grant 2131853. APW was supported by DOE award DE-SC0022302. We acknowledge AmeriFlux sites BRG, Ha1, Ho1, Ho2, Me6, MMS, NC2, NC3, NR1, Ro4, Seg, Ses, SRG, SRM, Syv, Ton, UMB, UMd, Var, Vcm, Vcp, Vcs, WCr, Whs, Wjs, and Wkg and the tower PIs for their data records. Funding for AmeriFlux data resources and core site data was provided by the U.S. Department of Energy's Office of Science. USDA is an equal-opportunity employer and provider. Thanks to C. Jerzak for fruitful statistical discussions, K. Novick for suggesting surface temperature analyses, and two anonymous referees for their careful reviews.

References

Abatzoglou, J. T., Dobrowski, S. Z., Parks, S. A., & Hegewisch, K. C. (2018). TerraClimate, a high-resolution global dataset of monthly climate and climatic water balance from 1958–2015. *Scientific Data*, *5*(1), 170191. https://doi.org/10.1038/sdata.2017.191

Aguirre, B. A., Hsieh, B., Watson, S. J., & Wright, A. J. (2021). The experimental manipulation of atmospheric drought: Teasing out the role of microclimate in biodiversity experiments. *Journal of Ecology*, *109*(5), 1986–1999. https://doi.org/10.1111/1365-2745.13595

Akaike, H. (1974). A new look at the statistical model identification. *IEEE Transactions on Automatic Control*, *19*(6), 716–723. https://doi.org/10.1109/TAC.1974.1100705

Assmann, S. M., Snyder, J. A., & Lee, Y. J. (2000). ABA-deficient (*aba1*) and ABA-insensitive (*abi1-1, abi2-1*) mutants of *Arabidopsis* have a wild-type stomatal response to humidity. *Plant, Cell and Environment*, *23*(4), 387–395. https://doi.org/10.1046/j.1365-3040.2000.00551.x

Barron-Gafford, G. A., Grieve, K. A., & Murthy, R. (2007). Leaf- and stand-level responses of a forested mesocosm to independent manipulations of temperature and vapor pressure deficit. *New Phytologist*, *174*(3), 614–625. https://doi.org/10.1111/j.1469-8137.2007.02035.x

Bauerle, W. L., Whitlow, T. H., Setter, T. L., & Vermeylen, F. M. (2004). Abscisic acid synthesis in *Acer rubrum* L. leaves—A vapor-pressure-deficit-mediated response. *Journal of the American Society for Horticultural Science*, *129*(2), 182–187. https://doi.org/10.21273/JASHS.129.2.0182

Bernacchi, C. J., Pimentel, C., & Long, S. P. (2003). *In vivo* temperature response functions of parameters required to model RuBP-limited photosynthesis. *Plant, Cell and Environment*, *26*(9), 1419–1430. https://doi.org/10.1046/j.0016-8025.2003.01050.x

Bernacchi, C. J., Singsaas, E. L., Pimentel, C., Portis Jr, A. R., & Long, S. P. (2001). Improved temperature response functions for models of Rubisco-limited photosynthesis. *Plant, Cell and Environment*, *24*(2), 253–259. https://doi.org/10.1111/j.1365-3040.2001.00668.x

Berry, J., & Bjorkman, O. (1980). Photosynthetic response and adaptation to temperature in higher plants. *Annual Review of Plant Physiology*, *31*(1), 491–543. https://doi.org/10.1146/annurev.pp.31.060180.002423

Burnham, K. P., & Anderson, D. R. (2004). Multimodal inference: Understanding AIC and BIC in model selection. *Sociological Methods and Research*, *33*(2), 261–304. https://doi.org/10.1177/0049124104268644

Campbell, G. S., & Norman, J. M. (1998). *An introduction to environmental biophysics* (2nd ed.). Springer. https://doi.org/10.1007/978-1-4612-1626-1

Canty, A., & Ripley, B. (2021). Boot: Bootstrap R (S-plus) functions [Computer Software]. *R package version 1.3-28*. Retrieved from https://cran.r-project.org/web/packages/boot/index.html

Cernusak, L. A., Ubierna, N., Jenkins, M. W., Garrity, S. R., Rahn, T., Powers, H. H., et al. (2018). Unsaturation of vapour pressure inside leaves of two conifer species. *Scientific Reports*, *8*(1), 7667. https://doi.org/10.1038/s41598-018-25838-2

Chu, H., & Hukfens, K. (2021). The amerifluxr package: An interface with AmeriFlux data services [Computer Software]. *R package version 1.0.0*. Retrieved from https://cloud.r-project.org/web/packages/amerifluxr/index.html

Chu, H., Luo, X., Ouyang, Z., Chan, W. S., Dengel, S., Biraud, S. C., et al. (2021). Representativeness of eddy-covariance flux footprints for areas surrounding AmeriFlux sites. *Agricultural and Forest Meteorology*, *301–302*, 108350. https://doi.org/10.1016/j.agrformet.2021.108350

Dannenberg, M. P., Yan, D., Barnes, M. L., Smith, W. K., Johnston, M. R., Scott, R. L., et al. (2022). Exceptional heat and atmospheric dryness amplified losses of primary production during the 2020 U.S. Southwest hot drought. *Global Change Biology*, *28*, 4794–4806. https://doi.org/10.1111/gcb.16214

Day, M. E. (2000). Influence of temperature and leaf-to-air vapor pressure deficit on net photosynthesis and stomatal conductance in red spruce (*Picea rubens*). *Tree Physiology*, *20*(1), 57–63. https://doi.org/10.1093/treephys/20.1.57

Ding, Y., Li, Z., & Peng, S. (2020). Global analysis of time-lag and -accumulation effects of climate on vegetation growth. *International Journal of Applied Earth Observation and Geoinformation*, *92*, 102179. https://doi.org/10.1016/j.jag.2020.102179

Famiglietti, J. S., Ryu, D., Berg, M. L., Rodell, M., & Jackson, T. J. (2008). Field observations of soil moisture variability across scales. *Water Resources Research*, *44*(1), W01423. https://doi.org/10.1029/2006WR005804

Farquhar, G. D., Von Caemmerer, S., & Berry, J. A. (1980). A biochemical model of photosynthetic CO_2 assimilation in leaves of C3 species. *Planta*, *149*(1), 78–90. https://doi.org/10.1007/BF00386231

Ficklin, D. L., & Novick, K. A. (2017). Historic and projected changes in vapor pressure deficit suggest a continental-scale drying of the United States atmosphere. *Journal of Geophysical Research*, *122*(4), 2061–2079. https://doi.org/10.1002/2016JD025855

Fu, Z., Ciais, P., Prentice, I. C., Gentine, P., Makowski, D., Bastos, A., et al. (2022). Atmospheric dryness reduces photosynthesis along a large range of soil water deficits. *Nature Communications*, *13*(1), 989. https://doi.org/10.1038/s41467-022-28652-7

Grossiord, C., Buckley, T. N., Cernusak, L. A., Novick, K. A., Poulter, B., Siegwolf, R. T. W., et al. (2020). Plant responses to rising vapor pressure deficit. *New Phytologist*, *226*(6), 1550–1566. https://doi.org/10.1111/nph.16485

Humphrey, V., Berg, A., Ciais, P., Gentine, P., Jung, M., Reichstein, M., et al. (2021). Soil moisture–atmosphere feedback dominates land carbon uptake variability. *Nature*, *592*, 65–69. https://doi.org/10.1038/s41586-021-03325-5

Inoue, T., Sunaga, M., Ito, M., Yuchen, Q., Matsushima, Y., Sakoda, K., & Yamori, W. (2021). Minimizing VPD fluctuations maintains higher stomatal conductance and photosynthesis, resulting in improvement of plant growth in lettuce. *Frontiers in Plant Science*, *12*, 646144. https://doi.org/10.3389/fpls.2021.646144

Johnston, M. R., Andreu, A., Verfaillie, J., Baldocchi, D., & Moorcroft, P. R. (2022). What lies beneath: Vertical temperature heterogeneity in a Mediterranean woodland savanna. *Remote Sensing of Environment*, *274*, 112950. https://doi.org/10.1016/j.rse.2022.112950

Juang, J.-Y., Katul, G., Siqueira, M., Stoy, P., & Novick, K. (2007). Separating the effects of albedo from eco-physiological changes on surface temperature along a successional chronosequence in the southeastern United States. *Geophysical Research Letters*, *34*(21), L21408. https://doi.org/10.1029/2007GL031296

Lange, O. L., Lösch, R., Schulze, E.-D., & Kappen, L. (1971). Responses of stomata to changes in humidity. *Planta*, *100*(1), 76–86. https://doi.org/10.1007/BF00386887

Lansu, E. M., Van Heerwaarden, C. C., Stegehuis, A. I., & Teuling, A. J. (2020). Atmospheric aridity and apparent soil moisture drought in European forest during heat waves. *Geophysical Research Letters*, *47*(6), e2020GL087091. https://doi.org/10.1029/2020GL087091

Li, F., Xiao, J., Chen, J., Ballantyne, A., Bing Li, K. J., Abraha, M., & John, R. (2023). Global water use efficiency saturation due to increased vapor pressure deficit. *Science*, *381*, 672–677. https://doi.org/10.1126/science.adf5041

Li, S., & Liu, F. (2022). Vapour pressure deficit and endogenous ABA level modulate stomatal responses of tomato plants to soil water deficit. *Environmental and Experimental Botany*, *199*, 104889. https://doi.org/10.1016/j.envexpbot.2022.104889

Lihavainen, J., Ahonen, V., Keski-Saari, S., Kontunen-Soppela, S., Oksanen, E., & Keinänen, M. (2016). Low vapour pressure deficit affects nitrogen nutrition and foliar metabolites in silver birch. *Journal of Experimental Botany*, *67*(14), 4353–4365. https://doi.org/10.1093/jxb/erw218

Lihavainen, J., Ahonen, V., Keski-Saari, S., Sõber, A., Oksanen, E., & Keinänen, M. (2017). Low vapor pressure deficit reduces glandular trichome density and modifies the chemical composition of cuticular waxes in silver birch leaves. *Tree Physiology*, *37*(9), 1166–1181. https://doi.org/10.1093/treephys/tpx045

Lihavainen, J., Keinänen, M., Keski-Saari, S., Kontunen-Soppela, S., Sõber, A., & Oksanen, E. (2016). Artificially decreased vapour pressure deficit in field conditions modifies foliar metabolite profiles in birch and aspen. *Journal of Experimental Botany*, *67*(14), 4367–4378. https://doi.org/10.1093/jxb/erw219

Lin, Y.-S., Medlyn, B. E., & Ellsworth, D. S. (2012). Temperature responses of leaf net photosynthesis: The role of component processes. *Tree Physiology*, *32*(2), 219–231. https://doi.org/10.1093/treephys/tpr141

Liu, L., Gudmundsson, L., Hauser, M., Qin, D., Li, S., & Seneviratne, S. I. (2020). Soil moisture dominates dryness stress on ecosystem production globally. *Nature Communications*, *11*, 4892. https://doi.org/10.1038/s41467-020-18631-1

Marchin, R. M., Broadhead, A. A., Bostic, L. E., Dunn, R. R., & Hoffmann, W. A. (2016). Stomatal acclimation to vapour pressure deficit doubles transpiration of small tree seedlings with warming. *Plant, Cell and Environment*, *39*(10), 2221–2234. https://doi.org/10.1111/pce.12790

McAdam, S. A. M., & Brodribb, T. J. (2015). The evolution of mechanisms driving the stomatal response to vapor pressure deficit. *Plant Physiology*, *167*(3), 833–843. https://doi.org/10.1104/pp.114.252940

McAdam, S. A. M., Sussmilch, F. C., & Brodribb, T. J. (2016). Stomatal responses to vapour pressure deficit are regulated by high speed gene expression in angiosperms. *Plant, Cell and Environment*, *39*(3), 485–491. https://doi.org/10.1111/pce.12633

Merilo, E., Yarmolinsky, D., Jalakas, P., Parik, H., Tulva, I., Rasulov, B., et al. (2018). Stomatal VPD response: There is more to the story than ABA. *Plant Physiology*, *176*(1), 851–864. https://doi.org/10.1104/pp.17.00912

Novick, K. A., Ficklin, D. L., Grossiord, C., Konings, A. G., Martínez-Vilalta, J., Sadok, W., et al. (2024). The impacts of rising vapor pressure deficit in natural and managed ecosystems. *Plant, Cell and Environment*, 1–24. https://doi.org/10.1111/pce.14846

Novick, K. A., Ficklin, D. L., Stoy, P. C., Williams, C. A., Bohrer, G., Oishi, A. C., et al. (2016). The increasing importance of atmospheric demand for ecosystem water and carbon fluxes. *Nature Climate Change*, *6*, 1023–1027. https://doi.org/10.1038/nclimate3114

Ogle, K., Barber, J. J., Barron-Gafford, G. A., Bentley, L. P., Young, J. M., Huxman, T. E., et al. (2015). Quantifying ecological memory in plant and ecosystem processes. *Ecology Letters*, *18*(3), 221–235. https://doi.org/10.1111/ele.12399

Olson, M. E., Anfodillo, T., Rosell, J. A., & Martínez-Méndez, N. (2020). Across climates and species, higher vapour pressure deficit is associated with wider vessels for plants of the same height. *Plant, Cell and Environment*, *43*(12), 3068–3080. https://doi.org/10.1111/pce.13884

Oren, R., Sperry, J. S., Katul, G. G., Pataki, D. E., Ewers, B. E., Phillips, N., & Schäfer, K. V. R. (1999). Survey and synthesis of intra- and interspecific variation in stomatal sensitivity to vapour pressure deficit. *Plant, Cell and Environment*, *22*(12), 1515–1526. https://doi.org/10.1046/j.1365-3040.1999.00513.x

Papale, D., Reichstein, M., Aubinet, M., Canfora, E., Bernhofer, C., Kutsch, W., et al. (2006). Towards a standardized processing of Net Ecosystem Exchange measured with eddy covariance technique: Algorithms and uncertainty estimation. *Biogeosciences*, *3*, 571–583. https://doi.org/10.5194/bg-3-571-2006

R Core Team. (2021). R: A language and environment for statistical computing [Computer Software]. https://www.R-project.org/

Reichle, R., De Lannoy, G., Koster, R. D., Crow, W. T., Kimball, J. S., Liu, Q., & Bechtold, M. (2022). SMAP L4 global 3-hourly 9 km EASE-grid surface and root zone soil moisture geophysical data, version 7 [Dataset]. *NASA National Snow and Ice Data Center Distributed Active Archive Center*. https://doi.org/10.5067/EVKPQZ4AFC4D

Roby, M. C., Scott, R. L., & Moore, D. J. P. (2020). High vapor pressure deficit decreases the productivity and water use efficiency of rain-induced pulses in semiarid ecosystems. *JGR Biogeosciences*, *125*(10), e2020JG005665. https://doi.org/10.1029/2020JG005665

Sadok, W., Lopez, J. R., & Smith, K. P. (2021). Transpiration increases under high-temperature stress: Potential mechanisms, trade-offs and prospects for crop resilience in a warming world. *Plant, Cell and Environment*, *44*(7), 2102–2116. https://doi.org/10.1111/pce.13970

Schönbeck, L. C., Schuler, P., Lehmann, M. M., Mas, E., Mekarni, L., Pivovaroff, A. L., et al. (2022). Increasing temperature and vapour pressure deficit lead to hydraulic damages in the absence of soil drought. *Plant, Cell & Environment*, *45*(11), 3275–3289. https://doi.org/10.1111/pce.14425

Shirke, P. A. (2004). Influence of leaf-to-air vapour pressure deficit (VPD) on the biochemistry and physiology of photosynthesis in *Prosopis juliflora*. *Journal of Experimental Botany*, *55*(405), 2111–2120. https://doi.org/10.1093/jxb/erh229

Sinclair, T., Fiscus, E., Wherley, B., Durham, M., & Rufty, T. (2007). Atmospheric vapor pressure deficit is critical in predicting growth response of "cool-season" grass *Festuca arundinacea* to temperature change. *Planta*, *227*, 273–276. https://doi.org/10.1007/s00425-007-0645-5

Stevens, A., & Ramirez-Lopez, L. (2022). prospectr: Miscellaneous functions for processing and sample selection of spectroscopic data [Computer software]. *R package version 0.2.3*. Retrieved from https://cran.r-project.org/web/packages/prospectr/vignettes/prospectr.html

Sulman, B. N., Roman, D. T., Yi, K., Wang, L., Phillips, R. P., & Novick, K. A. (2016). High atmospheric demand for water can limit forest carbon uptake and transpiration as severely as dry soil. *Geophysical Research Letters*, *43*(18), 9686–9695. https://doi.org/10.1002/2016GL069416

Thieurmel, B., & Elmarhraoui, A. (2019). suncalc: Compute sun position, sunlight phases, moon position and lunar phase [Computer software]. *R package version 0.5.0*. Retrieved from https://cran.r-project.org/web/packages/suncalc/index.html

Urban, J., Ingwers, M., McGuire, M. A., & Teskey, R. O. (2017). Stomatal conductance increases with rising temperature. *Plant Signaling and Behavior*, *12*(8), e1356534. https://doi.org/10.1080/15592324.2017.1356534

von Caemmerer, S., & Evans, J. R. (2015). Temperature responses of mesophyll conductance differ greatly between species. *Plant, Cell and Environment*, *38*(4), 629–637. https://doi.org/10.1111/pce.12449

Williams, A. P., Allen, C. D., Macalady, A. K., Griffin, D., Woodhouse, C. A., Meko, D. M., et al. (2013). Temperature as a potent driver of regional forest drought stress and tree mortality. *Nature Climate Change*, *3*, 292–297. https://doi.org/10.1038/nclimate1693

Williams, A. P., Seager, R., Berkelhammer, M., Macalady, A. K., Crimmins, M. A., Swetnam, T. W., et al. (2014). Causes and implications of extreme atmospheric moisture demand during the record-breaking 2011 wildfire season in the southwestern United States. *Journal of Applied Meteorology and Climatology*, *53*(12), 2671–2684. https://doi.org/10.1175/JAMC-D-14-0053.1

Wood, S. (2017). *Generalized additive models: An introduction with R* (2nd ed.). CRC Press. https://doi.org/10.1201/9781315370279

Wood, S. (2021). mgcv: Mixed GAM computation vehicle with automatic smoothness estimation [Computer software]. *R package version 1.8-38*. Retrieved from https://cran.r-project.org/web/packages/mgcv/index.html

Wutzler, T., Lucas-Moffat, A., Migliavacca, M., Knauer, J., Sickel, K., Šigut, L., et al. (2018). Basic and extensible post-processing of eddy covariance flux data with REddyProc. *Biogeosciences*, *15*(16), 5015–5030. https://doi.org/10.5194/bg-15-5015-2018

Wutzler, T., Reichstein, M., Moffat, A. M., & Migliavacca, M. (2021). REddyProc: Post processing of (half-)hourly eddy-covariance measurements [Computer software]. *R package version 1.3.1*. Retrieved from https://cran.r-project.org/web/packages/REddyProc/index.html

Yadav, V., Mueller, K. L., Dragoni, D., & Michalak, A. M. (2010). A geostatistical synthesis study of factors affecting gross primary productivity in various ecosystems of North America. *Biogeosciences*, *7*, 2655–2671. https://doi.org/10.5194/bg-7-2655-2010

Yuan, W., Zheng, Y., Piao, S., Ciais, P., Lombardozzi, D., Wang, Y., et al. (2019). Increased atmospheric vapor pressure deficit reduces global vegetation growth. *Science Advances*, *5*(8), eaax1396. https://doi.org/10.1126/sciadv.aax1396

Zhang, D., Du, Q., Zhang, Z., Jiao, X., Song, X., & Li, J. (2017). Vapour pressure deficit control in relation to water transport and water productivity in greenhouse tomato production during summer. *Scientific Reports*, *7*(1), 43461. https://doi.org/10.1038/srep43461

Zhang, Q., Ficklin, D. L., Manzoni, S., Wang, L., Way, D., Phillips, R. P., & Novick, K. A. (2019). Response of ecosystem intrinsic water use efficiency and gross primary productivity to rising vapor pressure deficit. *Environmental Research Letters*, *14*(7), 074023. https://doi.org/10.1088/1748-9326/ab2603

Zhong, Z., He, B., Wang, Y.-P., Chen, H. W., Chen, D., Fu, Y. H., et al. (2023). Disentangling the effects of vapor pressure deficit on northern terrestrial vegetation productivity. *Science Advances*, *9*(32), eadf316. https://doi.org/10.1126/sciadv.adf3166

Zhou, S., Zhang, Y., Park Williams, A., & Gentine, P. (2019). Projected increases in intensity, frequency, and terrestrial carbon costs of compound drought and aridity events. *Science Advances*, *5*(1), eaau5740. https://doi.org/10.1126/sciadv.aau5740

Zweifel, R., Sterck, F., Braun, S., Buchmann, N., Eugster, W., Gessler, A., et al. (2021). Why trees grow at night. *New Phytologist*, *231*(6), 2174–2185. https://doi.org/10.1111/nph.17552

References From the Supporting Information

Ren, K., & Russell, K. (2021). formattable: Create "formattable" data structures [Computer software]. *R package version 0.2.1*. Retrieved from https://cran.r-project.org/web/packages/formattable/index.html